

Quantum Mechanical Calculation of the Optical Absorption of Silver and Gold Nanoparticles by Density Functional Theory

Elham Gharibshahi and Elias Saion

Department of Physics, University Putra Malaysia, 34300 UPM Serdang, Selangor, Malaysia

Abstract: Problem statement: Metal nanoparticles confine the motion of conduction electrons and exhibit a strong optical absorption of electromagnetic radiation in the UV-vis-NIR region. The absorption is classically derived from the collective oscillations of free electrons in a metallic nanostructure as a consequence of incident electromagnetic radiation polarizing the particle optically embedded in a dielectric matrix. These oscillations, known as the localized surface Plasmon resonance has been modelled by Gustav Mie in 1908 using the Maxwell's equations. Nevertheless, the electrodynamics approach cannot account for the electronic transitions often displayed in experiment as a broad UV-vis optical absorption spectrum originated from the conduction electrons of metal nanoparticles. A quantum mechanical approach is required to address the optical absorption spectra of metal nanoparticles systemically. **Approach:** In this study, an attempt was made to calculate the optical absorption spectra of conduction electrons of metal nanoparticle quantum mechanically using the density functional theory. The particle was an isolated spherical metal nanoparticle containing N atoms confined in a face-centered cubic lattice structure. When light strikes the particle, the occupied ground-state conduction electrons absorbed the energy and excite to the unoccupied higher energy-state of the conduction band. In this development, we used time-independent Schrodinger equation for the ground-state energy of Thomas-Fermi-Dirac-Weizsacker atomic model for the total energy functional and the density function in the Euler-Lagrange equation is algebraically substituted with the absorption function. The total energy functional was computed numerically for silver and gold nanoparticles at various diameters. **Results:** The results showed broad absorption spectra derived from the occupied ground-state conduction electrons at the orbital $\{n = 5 \text{ and } l = 0 \text{ or } 5s\}$ for silver and $\{n = 6 \text{ and } l = 0 \text{ or } 6s\}$ for gold, which excite to the unoccupied higher energy of conduction band at the orbital $\{n \geq 6 \text{ and } l = 0 \text{ or } 1\}$ for silver and $\{n \geq 7 \text{ and } l = 0 \text{ or } 1\}$ for gold. A nonlinear red-shift of the absorption peak λ_{\max} , appearing at 404.79, 408.36, 412.55, 415.73, 418.42 and 420.96 nm for silver and at 510.28, 520.91, 533.11, 542.35, 549.74 and 556.04 nm for gold when the particle diameter varies at 4, 5, 7, 10, 15 and 25 nm respectively. The quantum confinement effect of the conduction bands is stronger for silver and gold nanoparticles of less than about 20 nm in diameter. **Conclusion:** The optical absorption spectra of silver and gold nanoparticles have been successfully calculated using a quantum treatment and this calculation could be extended to other transition metal nanoparticles of interest in nanoscience and nanotechnology.

Key words: Metal nanoparticles, optical absorption theory, quantum mechanical, density functional theory, numerical calculation

INTRODUCTION

Metal nanoparticles, typically 1-100 nm in dimension and containing 10^2 - 10^8 atoms demonstrate different physical and chemical properties from their bulk and atomic counterparts due to the surface and quantum confinement effects (Banfi *et al.*, 1998; Banyai *et al.*, 1988; Takagahara, 1989). They have attracted considerable attention owing to their potential applications in such as catalysis (Zhong *et al.*, 2010),

optics (Kambhampati and Knoll, 1999), optoelectronics (Tanabe, 2007), spectroscopy (Chen *et al.*, 2007; Cannone *et al.*, 2007), biomedical applications (Khlebtsov and Dykman, 2010) and electrochemical sensors (Korotcenkov *et al.*, 2009). Noble metal nanoparticles of silver (Ag) and gold (Au) confine the motion of free electrons in conduction band and exhibit a strong optical absorption of electromagnetic radiation in the UV-vis-NIR region. This phenomenon has been a challenge to scientists for the last one hundred years.

Corresponding Author: Elham Gharibshahi, Department of Physics, University Putra Malaysia, 34300 UPM Serdang, Selangor, Malaysia

According to the classical electrodynamics theory, the absorption is derived from the collective oscillations of free electrons in metallic nanostructures as a consequence of incident electromagnetic radiation polarizing the particles. These oscillations, known as the Localized Surface Plasmon Resonance (LSPR), are unique to metallic nanostructures and their resonance frequency is dependent on the particle characteristics such as the size, shape and chemical composition and the surrounding medium's dielectric properties.

Light extinction in a single spherical nanoparticle of arbitrary size embedded in an optically dielectric matrix has been modelled by Mie (1908) using the Maxwell's equations. The theory provides excellent results for very small nanoparticles of few nanometres in diameter. Several methods have been developed to determine the optical properties of non-spherical particles based on the electromagnetic theory (Bruzzone *et al.*, 2003; Okamoto and Yamaguchi, 2003; Noguez, 2005; Renteria and Garcia-Macedo, 2006). Nevertheless, the electrodynamics-based theories cannot account for the energy discretization of conduction electrons, which is the fundamental electronic property of metal nanoparticles.

A more satisfying treatment of light interaction with conduction electrons of metal nanoparticles requires a quantum theory consideration. Considerable efforts have been made to calculate the optical absorption and excitation of the valence electrons in metal nanoparticles based on the Time-Dependent Density Functional Theory (TD-DFT) (Hakkinen and Moseler, 2004; Sarasola *et al.*, 2004; Negrut *et al.*, 2006; Samal and Harbola, 2006; Aikens *et al.*, 2008; Gonzalez and Noguez, 2007; Huang and Carter, 2008; Chen and Zhou, 2008; Zheng *et al.*, 2009). The optical absorption spectra of metal nanoparticles can be determined from the ground-state density through the Hamiltonian operator because it characterizes all of the energy states of a system. However, quantum mechanical approach to quantify the optical absorption of conduction electrons of metal nanoparticles has not been addressed systemically. The discrete absorption spectra of conduction electron transitions have not been seen in optical measurements. Instead, UV-visible absorption spectra of metal nanoparticles are often displayed as a broad spectrum originated from the conduction electron transitions with exceptionally degenerate states. This is in marked contrast with absorption properties of the valence electrons of metal nanoparticles such as luminescence (Drachev *et al.*, 2004) and fluorescence (Roque *et al.*, 2006), where the quantized states are readily observed due to well-defined energy gap between two occupied energy

states. In metal nanoparticles, the electron-hole interaction is screened off and the conduction electrons behave as nearly free.

The present study describes a fully quantum mechanical calculation of the optical absorption spectra of Ag and Au nanoparticles based on time-independent DFT. The particle is an isolated single solid metal nanosphere containing N atoms arranged in a face-centered cubic lattice structure. The total energy functional is the ground-state energy functional of the Thomas-Fermi-Dirac-Weizsacker atomic model to allow for the ground-state conduction electron density to be finite at the lowest energy state of the conduction band. The optical absorption of conduction electrons may be calculated by DFT because there is a relationship between the electron density function and the absorption function. In this development, the electronic density function in the final Euler-Lagrangian equation is algebraically substituted with the absorption function. Our study includes the calculation of Lagrange multipliers, lattice constants, nuclear and electronic potentials, ground-state wave vectors, number of atoms and conduction electrons in a given particle size and optical absorption spectrum.

MATERIALS AND METHODS

Theoretical and numerical simulation: The schematic version of the band structure of metal nanoparticle is shown in Fig. 1. When light strikes the particle, the occupied ground-state conduction electrons absorbed photon energy and excite to the unoccupied higher energy-state of the conduction band. These events are seen in UV-visible absorption spectra measurements and can be used to study the conduction band electronic structures of the metallic nanoparticles.

In quantum mechanical calculation, Hohenberg-Kohn-Sham DFT (Thomas, 1927) has been most widely used to study the electronic structures of many-electron systems such as nanostructures. The early foundations of DFT are due to the Hohenberg and Kohn theorem and Kohn-Sham equations, where the ground state electron density $\rho(r)$ is the basic variable, from which all ground state properties could be derived. For optical absorption of metal nanoparticles, the ground-state energy functional $E[\rho(r)]$ may be taken from the Thomas-Fermi-Dirac-Weizsacker atomic model (Thomas, 1927; Kohn and Sham, 1965; Fermi, 1927; Dirac, 1930; Von Weizsacker, 1935), written as:

$$E[\rho(r)] = T_{TF}[\rho(r)] + \lambda T_W[\rho(r)] + \int \rho(r)v(r)dr + V_{ce}[\rho(r)] \quad (1)$$

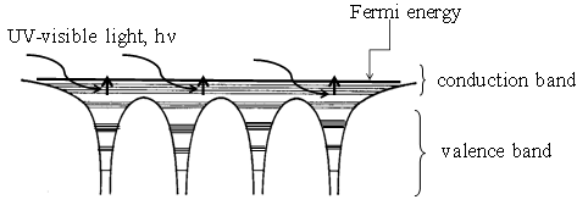


Fig. 1: Schematic version of the energy band structure of a metal nanoparticle showing only four atoms of Ag nanoparticles. The optical absorption may be represented by absorption of UV-visible light by the occupied ground-state conduction electrons at the orbital $\{n = 5 \text{ and } l = 5\}$ or $5s$ electron state and promoted to the unoccupied higher energy states of the conduction band at the minimum orbital of either $\{n = 6 \text{ and } l = 0 \text{ or } 6s\}$ state or $\{n = 6 \text{ and } l = 1 \text{ or } 6p\}$ state according to quantum number $\Delta n \geq 1$ and $\Delta n = 0, 1$. The number of the ground-state conduction electrons increases corresponding to the number of atoms that made up the sizes of the nanoparticles

The first term, $T_{TF}[\rho(r)]$ is the kinetic energy of the Thomas-Fermi (TF) model in its original formulation of a local density approximation and expressed as a function of electron density $\rho(r)$ for an infinite number of homogenous free electron gas systems at a given coordinate r , given by:

$$T_{TF}[\rho(r)] = C_k \int \rho(r)^{5/3} dr \quad (2)$$

Where:

$$C_k = \frac{3}{10} \frac{h}{m} (3\pi^2)^{2/3}$$

$\lambda T_w[\rho(r)]$ = The Von Weizsacker (1935) correction to the kinetic energy of the TF model by inclusion exchange and correlation energy terms for the inhomogeneity of the electron density as a gradient correction about the uniform electron gas

This is the correct kinetic energy functional for metal nanoparticles where the conduction electrons resemble a one-electron or two-electron Hartee-Fock atom, given by:

$$T_w[\rho(r)] = \frac{1}{8} \frac{h^2}{m} \int \frac{|\tilde{\nabla}\rho(r)|^2}{\rho(r)} dr \quad (3)$$

The parameter λ may be obtained by some empirical arguments for the ground state energy (Chen

and Zhou, 2008; Yang, 1986; Engel and Dreizler, 1989; Chattaraj and Sengupta, 1997). The third term of Eq. 1 is the potential energy of the system and the fourth term, expressed as $V_{ee}[\rho(r)] = J[\rho(r)] - K_{TFD}[\rho(r)]$, is the potential energy functional for the effective electron-electron repulsion. $J[\rho(r)]$ is the classical Coulomb energy of electron-electron interactions and $K_{TFD}[\rho(r)]$ is the Thomas-Fermi-Dirac (TFD) model, which refers to the non-classical exchange-correlation energy of a homogenous free electron gas system defined as containing all remaining quantum effects not captured by J and kinetic energies T :

$$J[\rho(r, r')] = \frac{1}{2} \iint \frac{\rho(r)\rho(r')}{|r-r'|} dr dr' \quad (4)$$

and

$$K_{TFD}[\rho(r)] = C_e \int \rho(r)^{4/3} dr; C_e = e^2 \frac{3}{4} \left(\frac{3}{\pi}\right)^{1/3} \quad (5)$$

By taking atomic units $\hbar = m = e = c = 1$ throughout, the total energy functional, in the differential form to the second order is:

$$E[\rho] = C_k \int \rho(r)^{5/3} dr + \frac{\lambda}{8} \int \frac{|\tilde{\nabla}\rho(r)|^2}{\rho(r)} dr + \int \rho(r)v(r) dr + \frac{1}{2} \iint \frac{\rho(r)\rho(r')}{|r-r'|} dr dr' - C_e \int \rho(r)^{4/3} dr \quad (6)$$

The exact ground state energy of the metal nanoparticles is the global minimum value of $E[\rho(r)]$ and the density $\rho(r)$ that minimizes $E[\rho(r)]$ is the exact ground state density ρ_0 , namely:

$$E_0 = E[\rho_0] = \min\{E[\rho(r)] : \rho \geq 0, \int \rho(r) dr = N\} \quad (7)$$

Where:

E_0 = The exact ground state energy

$E[\rho_0]$ = The minimized energy functional (Hohenberg and Kohn, 1964)

N = The number of electrons in the conduction band

The ground-state electron density must satisfy the variational principle:

$$\delta\{E[\rho] - \mu[\int \rho(r) dr - N]\} = 0 \quad (8)$$

where, μ is the Lagrange multiplier associated with the normalized density functional. For completely degenerate conduction electrons at absolute zero temperature, μ is the Fermi energy. This yields the Euler-Lagrangian equation and is written as:

$$\mu = \frac{\delta E[\rho(r)]}{\delta \rho(r)} = v(r) + \frac{\delta T_{TF}}{\delta \rho(r)} + \lambda \frac{\delta T_w}{\delta \rho(r)} + \frac{\delta V_{ee}}{\delta \rho(r)} \quad (9)$$

The Euler-Lagrangian Eq. 6 may be presented in terms of functional derivatives:

$$\begin{aligned} & \frac{5}{3} C_k \int \rho(r)^{2/3} dr + \frac{\lambda}{8} \left[\frac{|\tilde{N}\rho(r)|^2}{\rho^2(r)} - 2 \frac{\tilde{N}^2 \rho(r)}{\rho(r)} \right] \\ & + v(r) + e^2 \int \frac{\rho(r)}{|r-r'|} dr - \frac{4}{3} C_e \int \rho(r)^{1/3} dr = \mu \end{aligned} \quad (10)$$

where, r , the displacement coordinate of the conduction electrons from the centre of nanosphere and is dependent on the Bohr radius a_0 , atomic number Z , the principle quantum number n and the angular quantum number l . For ground-state conduction electrons at absolute zero temperature, μ is the Fermi energy. We found that the density of conduction electrons $\rho(r)$ of an atom is a function of atomic number Z and absorption $\sigma(r)$ or $\rho(r) = \rho\{Z, \sigma(r)\}$. Since both $\rho(r)$ and $\sigma(r)$ are continuous functions, the transformation of the density functional energy $E[\rho(r)]$ to the absorption functional energy $E[\sigma(r)]$ can be made by algebraically substituting the electron density function in the Euler-Lagrangian Eq. 10 with the absorption function:

$$\begin{aligned} & \frac{\partial^2 \sigma(r)}{\partial r^2} + \frac{c_1}{\sigma(r)} \left(\frac{\partial \sigma(r)}{\partial r} \right)^2 + c_2 (v - \mu) \sigma(r) \\ & + c_3 \sigma(r)^{1/2} + c_4 = 0 \end{aligned} \quad (11)$$

where, c_1, c_2, c_3 and c_4 are constants. The final Euler-Lagrangian Eq. 11 is the second order differential equation in terms of the absorption function.

The absorption functional energy $E[\sigma(r)]$ of the conduction electrons is dependent on the particle type described by the atomic number, Fermi energy, potential energy and electron density, on the particle size described by the number of atoms that made up the spherical volume, lattice constant and ground-state wave vector and on the quantum number selection rules for the principle and angular quantum numbers. The transition $\Delta n \geq 1$ for the principle quantum number and

$\Delta l = 0, 1$ for angular quantum number, conduction electrons receive a plane electromagnetic wave x from photons and must overcome the ground-state electromagnetic wave vector k_n to promote to the higher energy states of the conduction band. The lattice constants a calculated for Ag and Au nanoparticles are 0.408 and 0.407 nm, respectively. The ground-state energy of the conduction electrons has the principle quantum number $n = 5$ and 6 for Ag and Au nanoparticles respectively. The Fermi levels μ calculated for Ag and Au atoms to be 5.49 and 5.53 eV respectively. By using Bloch's theorem and the Born-von Karman conditions, we reach the boundary conditions at the end points of the nanocrystal of $\sigma_0 = 0$ and $\sigma_N = 0$, where the two end points overlap to form a lattice loop. For numerical calculation, the absorption and wavelength in the Euler-Lagrangian equation are discretized (Yang, 1986) into σ_i and x_i , by:

$$\partial^2 \sigma(x) / \partial x^2 = (\sigma_{i+1} + \sigma_{i-1} - 2\sigma_i) / \Delta^2$$

and

$$\partial \sigma(x) / \partial x = (\sigma_{i+1} - \sigma_{i-1}) / 2\Delta$$

where, $i = 0, 1, 2, \dots, N$ are integers representing the number of atoms that made up the spherical volume of a given diameter. The multivariate equations may be solved numerically by a trapezoid integration method using the Newton iterative program with a mesh size, $\Delta = 0.01$. Numerical simulations are carried out on single particle of different sizes.

RESULTS AND DISCUSSION

Figure 2 depicts the calculated optical absorption spectra as a function of wavelength of the incident photons for a 4 nm Ag nanoparticle containing 50 atoms. The absorption spectra are derived from the occupied ground-state conduction electrons at the orbital 5s, which excite to the unoccupied higher-energy states of conduction band at the orbital ns or np or both with many possible transitions at $n \geq 6$ and $l = 0$ or 1. Here shown only for ten transitions from 5-10s, 13, 15, 20 and 25s ($n \geq 6, \Delta l = 0$) and from 5s to 10p, 13, 15, 20 and 25p ($n \geq 6, \Delta l = 1$). Each spectrum represents transitions made by 50 conduction electrons to produce an absorption peak of λ_{max} . It is interesting to note that despite many possible transitions, the discreteness of the conduction band does not clearly manifests itself because the absorption peak λ_{max} of each transition spectrum is very close to the other transitions.

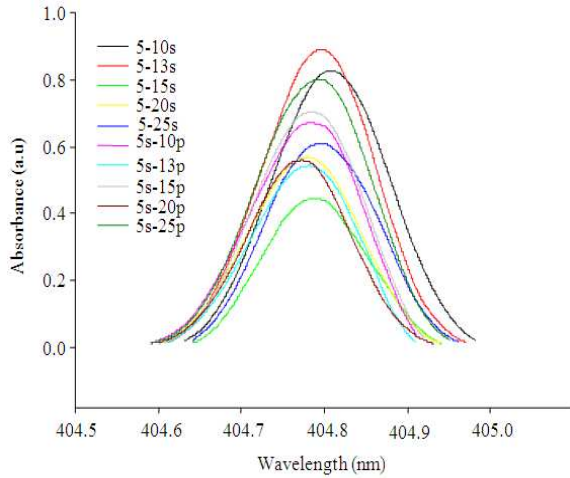


Fig. 2: Calculated optical absorption spectra of a 4 nm Ag nanoparticle, showing the absorption peaks of ten transitions from 5-10s, 13, 15, 20 and 25s ($n \geq 6$, $\Delta l = 0$) and from 5s to 10p, 13, 15, 20 and 25p ($n \geq 6$, $\Delta l = 1$). The energy bands of s-electrons and p-electrons at the higher energy states of the conduction band are confined very close to each other and any possible transitions with quantum number $n \geq 6$ and $\Delta l = 0$ or 1, produces the absorption peak revolves around $\lambda_{\max} = 404.79$ nm corresponds to the conduction band energy of 3.065 eV

The absorption peaks λ_{\max} of the transitions shown for 4 nm Ag nanoparticles appear in narrow wavelength regimes between 404.77 and 404.81 nm. It seems that the band gap between immediate electronic transitions (say for $\Delta n = 5, 8, 10, 15$ and 20) is insignificant. This means that at the higher energy states of the conduction band, the s-electrons and p-electrons are confined very close to each other and can overlap. This is because at the distance far from the particle center and close to the Fermi level, the nuclear potential of the conduction electrons is the weakest and any transition allowed by the quantum number selection rules will have degenerate states, i.e., the absorption energy equal to the conduction band energy. The final absorption spectrum of the Ag nanoparticle from all possible transitions is somewhat broadened but revolves around $\lambda_{\max} = 404.79$ nm corresponds to the conduction band energy of 3.065 eV.

Fig. 3 depicts the calculated optical absorption spectra of ten possible transitions as a function of incident photon wavelength for a 4 nm Au nanoparticle.

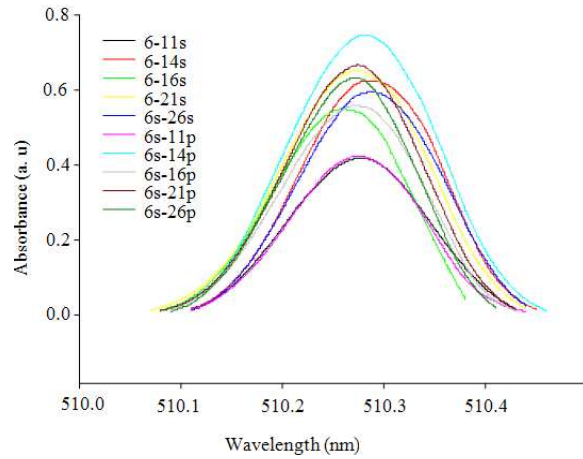


Fig. 3: Calculated optical absorption spectra of a 4 nm Au nanoparticle, showing the absorption peaks of ten transitions from 6-11s, 14, 16, 21 and 26s ($n \geq 7$, $\Delta l = 0$) and from 6s to 11p, 14, 16, 21 and 26p ($n \geq 7$, $\Delta l = 1$). The energy bands of s-electrons and p-electrons at the higher energy states of the conduction band are confined very close to each other and any possible transitions with quantum number $n \geq 7$ and $\Delta l = 0$ or 1 produces the absorption peak revolves around $\lambda_{\max} = 510.28$ nm corresponds to the conduction band energy of 2.432 eV

The spectra are derived from the ground-state conduction electrons from the orbital 6-11s, 14, 16, 21s and 26s ($n \geq 7$, $\Delta l = 0$) and from 6s to 11p, 14, 16, 21 and 26p ($n \geq 7$, $\Delta l = 1$). Similar to the situation of Ag nanoparticle, the absorption peaks λ_{\max} of Au nanoparticle appear in the narrow wavelength regime between 510.27 and 510.29 nm. The final absorption spectrum of the Au nanoparticle should be a more broader spectrum owing to many possible transitions allowed by quantum number selection rules ($n \geq 7$ and $\Delta l = 0$). For the 4 nm Au nanoparticle the absorption peak revolves around $\lambda_{\max} = 510.28$ nm corresponds to the conduction band energy of 2.432 eV.

A red-shift of the absorption peak based on LSPR in metal nanoparticles has been well documented (Pan *et al.*, 1993; Sakai *et al.*, 2009). We found that the absorption peaks λ_{\max} appear at 404.79, 408.36, 412.55, 415.73, 418.42 and 420.96 nm for Ag nanoparticles of diameters 4, 5, 7, 10, 15 and 25 nm respectively. The absorption spectra become higher and broaden with the increase in particle size. For Au nanoparticles the absorption peaks λ_{\max} appear at 510.28, 520.91, 533.11, 542.35, 549.74 and 556.04 nm for particle diameter of

4, 5, 7, 10, 15 and 25 nm respectively. An increase in the absorption peak λ_{\max} with the increase of particle sizes is attributed to the increase in the number of atoms that made up the particle sizes. There is an absorption peak red shift, which is longer for the smaller particle sizes than the larger sizes, indicating the absorption phenomenon of Ag and Au nanoparticles is nonlinearly size dependence (Pan *et al.*, 1993; Anno and Tanimoto, 2006).

The appearance of the absorption peak λ_{\max} at distinct regimes between Ag and Au nanoparticles for a given particle size is worth mentioning. The absorption peaks λ_{\max} for 4 nm Ag and Au nanoparticles appear at 404.79 and 510.28 nm, respectively, while for 25 nm Ag and Au nanoparticles they appear at 420.96 and 556.04 nm, respectively. The discrepancy in the absorption peaks of the two metallic systems is attributed to several factors, such as the multiplier parameter μ , lattice constant a , atomic number Z , nuclear potential and number of atoms. We noted that the Fermi energy and lattice constant of Ag and Au are about equal, but the absorption peaks λ_{\max} of the two systems appear at different wavelength regimes. The reason is that the nuclear potential of the system is proportional to the atomic number Z and inversely proportional to the radius, r . The numbers of proton of Ag and Au atoms are 47 and 79 respectively. Au nanoparticle has a stronger nuclear potential than Ag nanoparticle. Thus, the conduction electrons of Au nanoparticle are attracted stronger towards the center of the particle than Ag nanoparticle, reducing the size of the conduction band of Au nanoparticle than the Ag nanoparticle. Consequently, the absorption peak λ_{\max} of Au nanoparticle is longer than the Ag nanoparticle. We also observe that for nanoparticle diameters between 4 and 25 nm, the absorption peak λ_{\max} increases from 404.79-420.96 nm for Ag nanoparticles and from 510.28 and 556.04 nm for Au nanoparticles. An increase in the number of atoms produces larger particle sizes, which increase the nuclear potential energy of the system. An increase in the number of atoms produces larger particle sizes, which increase the nuclear potential energy of the system and thus decrease the conduction band by $1/r$. This increases the absorption peak as the particle size increases. This increases the absorption peak λ_{\max} as the particle size increases. In neighboring metallic systems, such as Pt and Au, which are different only by one conduction electron in each atom, we expect that the influence of the nuclear potential is not so dominant when compared to other factors such as the ground-state conduction electronic structure and multiplier parameter μ .

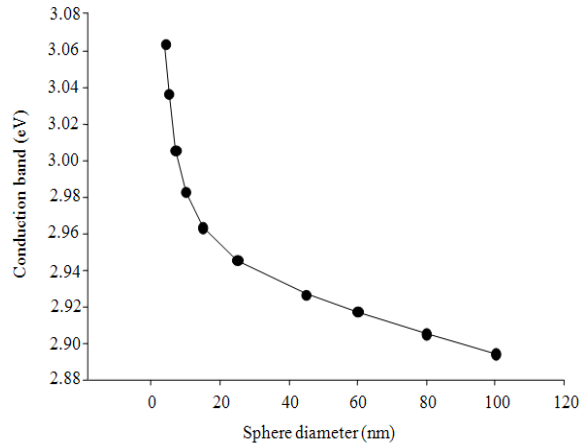


Fig. 4: Conduction band of Ag nanoparticles as a function of sphere diameter, showing the quantum confinement effect of the conduction band is stronger at the smaller particle sizes than the larger sizes

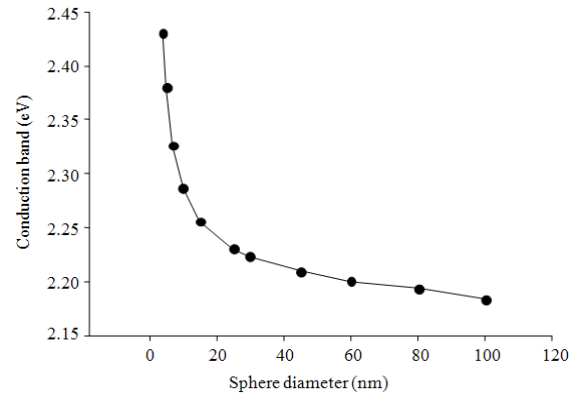


Fig. 5: Conduction band of Au nanoparticles as a function of sphere diameter, showing the quantum confinement effect of the conduction band is stronger at the smaller particle sizes than the larger sizes

Quantum confinement effects on some properties of nanostructures have been reported (Anno and Tanimoto, 2006; Haglund *et al.*, 1994; Pejova and Grozdanov, 2004). Figure 4 depicts the conduction band energy of the Ag nanoparticles as a function of diameter. It shows that as the particle diameter increases from 4-100 nm, the conduction band decreases from 3.065-2.895 eV. Figure 5 depicts the conduction band energy of Au nanoparticles at various diameters. As the particle diameter increases from 4-100 nm, the Au nanoparticle conduction band decreases from 2.432-2.183 eV. The change in conduction band is

very significant for the smaller particle sizes than the larger particle sizes. This means strong quantum confinement conduction band effects of the Ag and Au nanoparticles occurred for smaller particle sizes below about 20 nm. This effect is less significant with the larger particle sizes. This suggests that Ag and Au nanoparticles become more relevant in many applications at the smaller sizes because their conduction bands can be tuned more widely with smaller particle diameters.

CONCLUSION

In summary, we successfully used a quantum mechanical approach to simulate numerically the optical absorption spectra of the Ag and Au nanoparticles based upon time-independent DFT. The optical absorption is derived from light impinging on the metal nanoparticle causing the occupied ground-state conduction electrons to excite to the unoccupied higher energy states of the conduction band. The calculated absorption peaks λ_{\max} are sensitive to the particle type, which characterizes by the atomic number, Fermi energy, absorption function, potential energy of the system and absorption and electron density and on the particle size, which describes by the number of atoms and lattice constant. The absorption peaks λ_{\max} red-shift to the higher wavelengths by increasing the particle diameter and appear at 404.79, 408.36, 412.55, 415.73, 418.42 and 420.96 nm for Ag nanoparticles and at 510.28, 520.91, 533.11, 542.35, 549.74 and 556.04 nm for Au nanoparticles when simulated for diameter sizes of 4, 5, 7, 10, 15 and 25 nm respectively. The change in the absorption wavelength shift is substantial at the smaller particle sizes than the larger sizes. There is a strong quantum confinement effect on the conduction band energy for the smaller Ag and Au nanoparticles below about 20 nm. The quantum mechanical calculations of the optical absorption spectra, presented here for Ag and Au nanoparticles could be extended to other transition metal nanoparticles of interest in nanoscience and nanotechnology.

ACKNOWLEDGEMENT

This study was supported by the Ministry of Higher Education of Malaysia under the FRGS and RUGS grants.

REFERENCES

Aikens, C.M., S. Li and G.C. Schatz, 2008. From discrete electronic states to Plasmon: TDDFT optical absorption properties of Ag_n ($n = 10, 20, 35, 56, 84, 120$) tetrahedral clusters. *J. Phys. Chem. C*, 11: 11272-11279.

Anno, E. and M. Tanimoto, 2006. Size-dependent change in energy bands of nanoparticles of white tin. *Phys. Rev.*, 73: 155430-155436.

Banfi, G.P., V. Degiorgi and D. Ricard, 1998. Nonlinear optical properties of semiconductor nanocrystals. *Adv. Phys.*, 47: 447-510.

Banyai, L., Y.Z. Hu, M. Lindberg and S.W. Koch, 1988. Third-order optical nonlinearities in semiconductor microstructures. *Phys. Rev. B*, 38: 8142-8153.

Bruzzone, S., G.P. Arrighini and C. Guidotti, 2003. Theoretical study of the optical absorption behavior of Au/Ag core-shell nanoparticles. *Mater. Sci. Eng. C*, 23: 965-970.

Cannone, F., M. Collini, L. D'Alfonso, G. Baldini and G. Chirico *et al.*, 2007. Voltage regulation of fluorescence emission of single dyes bound to gold nanoparticles. *Nano Lett.*, 7: 1070-1075.

Chattaraj, P.K. and S. Sengupta, 1997. Dynamics of chemical reactivity indices for a many-electron system in its ground and excited states. *J. Phys. Chem. A*, 101: 7893-7900.

Chen, H. and A. Zhou, 2008. Orbital-free density functional theory for molecular structure calculations. *Num. Math.: Theory Method Appl.*, 1: 1-28.

Chen, Y., K. Munechika and D.S. Ginger, 2007. Dependence of fluorescence intensity on the spectral overlap between fluorophores and Plasmon resonant single silver nanoparticles. *Nano Lett.*, 7: 690-696.

Dirac, P.A.M., 1930. Note on exchange phenomena in the Thomas atom. *Math. Proc. Cambridge Philos. Soc.*, 26: 376-385.

Drachev, V.P., E.N. Khaliullin, K. Kim, F. Alzoubi and S.G. Rautian *et al.*, 2004. Quantum size effect in two-photon excited luminescence from silver nanoparticles. *Phys. Rev. B*, 69: 1-5.

Engel, E. and R.M. Dreizler, 1989. Extension of the Thomas-Fermi-Dirac-Weizsacker model: four-order gradient corrections to the kinetic energy. *J. Phys. B.: Atomic Mol. Opt. Phys.*, 22: 1901-1912.

Fermi, E., 1927. Un metodo statistico per la determinazione di alcune priorieta dell'atome. *Rend. Accad. Naz. Lincei*, 6: 602-607.

Gonzalez, A.L. and C. Noguez, 2007. Influence of morphology on the optical properties of metal nanoparticles. *J. Comp. Theor. Nanosci.*, 4: 231-238.

Haglund Jr., R.F., L. Yang, R.H. Magruder, C.W. White and R.A. Zuhr *et al.*, 1994. Nonlinear optical properties of metal-quantum-dot composites synthesized by ion implantation. *Nucl. Inst. Methods Phys. Res. B.: Beam Interact. Mater. Atoms*, 91: 493-504.

- Hakkinen, H. and M. Moseler, 2004. Symmetry and electronic structure of noble-metal nanoparticles and the role of relativity. *Phys. Rev. Lett.*, 93: 093401-1-4.
- Hohenberg, P. and W. Kohn, 1964. Inhomogeneous electron gas. *Phys. Rev.*, 136: 864-871.
- Huang, P. and E.A. Carter, 2008. Advances in correlated electronic structure methods for solids surfaces and nanostructures. *Ann. Rev. Phys. Chem.*, 59: 261-290.
- Kambhampati, D.K. and W. Knoll, 1999. Surface-Plasmon optical techniques. *Curr. Opin. Colloid Interface Sci.*, 4: 273-280.
- Khlebtsov, N.G. and L.A. Dykman, 2010. Optical properties and biomedical applications of plasmonic nanoparticles. *J. Quant. Spectrosc. Radiat. Transf.*, 111: 1-35.
- Kohn, W. and L.J. Sham, 1965. Self-consistent equations including exchange and correlation effects. *Phys. Rev.*, 140: 1133-1138.
- Korotcenkov, G., S.D. Han and J.R. Stetter, 2009. Review of electrochemical hydrogen sensors. *Chem. Rev.*, 10: 1402-1433.
- Mie, G., 1908. Beitrage zur Optik truber Medien speziell kolloidaler Metallosungen. *Annalen Der Physik.*, 25: 377-445.
- Negrut, D., M. Anitescu, A. El-Azab and P. Zapol, 2006. Quasicontinuum-like Reduction of DFT Calculations of nanostructures. *J. Nanosci. Nanotechnol.*, 8: 3729-3740.
- Noguez, C., 2005. Optical properties of isolated and supported metal nanoparticles. *Opt. Mater.*, 27: 1204-1211.
- Okamoto, T. and I. Yamaguchi, 2003. Optical absorption study of the surface Plasmon resonance in gold by self-assembly technique. *J. Phys. Chem. B.*, 38: 10321-10324.
- Pan, A., Z. Yang, H. Zheng, F. Liu and Y. Zhu *et al.*, 1993. Changeable position of SPR peak of Ag nanoparticles embedded in mesoporous SiO₂ glass by annealing treatment. *Applied Surface Sci.*, 205: 323-328.
- Pejova, B. and I. Grozdanov, 2004. Manifestations of three-dimensional confinement effects in the optical spectra of CdSe quantum dots in thin film form. *Mater. Lett.*, 58: 666-671.
- Renteria, V.M. and J. Garcia-Macedo, 2006. Modeling of optical absorption of silver prolate nanoparticles stabilized by Gemini surfactant. *Colloids Surf. A.*, 273: 1-3.
- Roque, J., N. Poolton, J. Molera, A. Smith and A.E. Pantos *et al.*, 2006. X-ray absorption and luminescence properties of metallic copper nanoparticles embedded in a glass matrix. *Phys. Stat. Solidi B.*, 243: 1337-1346.
- Sakai, N., Y. Fujiwara, M. Arai, K. Yu and T. Tatsuma, 2009. Electrodeposition of gold nanoparticles on ITO: Control of morphology and Plasmon resonance-based absorption and scattering. *J. Elect. Chem.*, 628: 7-15.
- Samal, P. and M.K. Harbola, 2006. Exploring foundations of time-independent density functional theory for excited states. *J. Phys. B.: Atomic Mol. Opt. Phys.*, 39: 4065-4080.
- Sarasola, A., R.H. Ritchie, E. Zaremba and P.M. Echenique, 2004. Density functional theory based stopping power for 3D and 2D systems. *Adv. Quant. Chem.*, 46: 1-28.
- Takagahara, T., 1989. Biexciton states in semiconductor quantum dots and their nonlinear optical properties. *Phys. Rev. B.*, 39: 10206-10231.
- Tanabe, K., 2007. Optical radiation efficiencies of metal nanoparticles for optoelectronic applications. *Mater. Lett.*, 61: 4573-4575.
- Thomas, L.H., 1927. The calculation of atomic fields. *Math. Proc. Cambridge Philos. Soc.*, 23: 542-548.
- Von Weizsacker, C.F., 1935. Zur Theorie der Kernmassen. *Zeitschrift fur Phys.*, 96: 431-458.
- Yang, W., 1986. Gradient correction in Thomas-Fermi theory. *Phys. Rev. A.*, 34: 4575-4585.
- Zheng, Y.B., Y.W. Yan, L. Jensen, L. Fang and B.K. Juluri *et al.*, 2009. Active molecular plasmonics: controlling Plasmon resonances with molecular switches. *Nano Lett.*, 9: 819-825.
- Zhong, C.J., J. Luo, B. Fang, B.N. Wanjala and P.N. Njoki *et al.*, 2010. Nanostructured catalysts in fuel cells. *Nanotechnology*, 21: 1-20.